ACS OMEGA

http://pubs.acs.org/journal/acsodf

Article

Theoretical Study on the Mechanism of Cobalt-Catalyzed C−O Silylation and Stannylation

Cheng-Xing Cui,* Jiali Peng, and Jun Jiang

Cite This: *ACS Omega* 2023, 8, 23791−23798

Read Online

ACCESS | Metrics & More | Article Recommendations | Supporting Information

ABSTRACT: Organosilicon and organotin compounds have been widely used in many fields, such as organic synthesis, materials science, and biochemistry, because of their unique physical and electronic properties. Recently, two novel compounds containing C−Si or C−Sn bonds have been synthesized. These compounds can be used for late modification of drug-like molecules such as probenecid, duloxetine, and fluoxetine derivatives. However, the detailed reaction mechanisms and the influencing factors that determine selectivity are still unclear. Moreover, several questions remain that are valuable to investigate further, such as (1) the influence of the solvent and the lithium salt on the reaction of the Si/Sn−Zn reagent, (2) the stereoselective functionalization of C−O bonds, and (3) the differences between silylation and stannylation. In the current study, we have explored the above issues with density functional theory and have found that stereoselectivity was most likely caused by the oxidative addition of cobalt to the C−O bond of alkenyl acetate with chelation assistance and that transmetalation was most likely the rate-determining step. For Sn−Zn reagents, the transmetalation was achieved by anion and cation pairs, whereas for Si−Zn reagents, the process was facilitated by Co−Zn complexes.

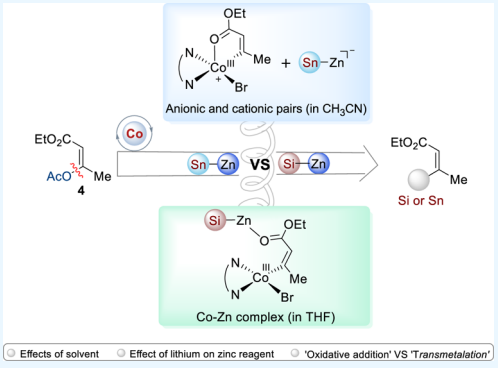

INTRODUCTION

Organosilicon compounds have been widely used in organic synthesis,[1,2] materials science,[3] and agricultural chemistry and have also played an increasing role in medicinal chemistry due to their slight physical and electronic changes, as a substitute for silane, bioisosteres of carbon, or other moieties.[4,5] Organotin compounds are important catalysts for the synthesis of polyurethanes composed of polyols and aliphatic isocyanates[6−9] and have attracted a lot of attention in recent years due to their unique properties in battery design.[10] Therefore, the synthesis of compounds containing C−Si and C−Sn bonds by experimental means has aroused chemists' thinking. As many contributions have reported, transition metal-catalyzed (TMC) cross-coupling is a powerful toolbox for manipulating C−X (X = heteroatom) bonds in the synthesis of agricultural chemicals, pharmaceuticals, and raw commodity chemicals.[11−17] Consequently, TMC could also be a potential tool for the construction of C−Si and C−Sn bonds.[18]

In recent years, Li and co-workers have reported a number of articles related to Zn reagents catalyzed by Co or Ni.[19−22] Not long ago, they reported that stereoselective tri- and tetrasubstituted alkenyl silane and stannanes were prepared by pregenerated cobalt-catalyzed cross-coupling of alkenyl acetates with solid Me_2PhSi-ZnOPiv·Li_2 (Cl)(OPiv) (**2**) (where Piv is pivalic acid) and (^{n}Bu)$_3$Sn−ZnCl·LiCl (**3**) under mild reaction conditions (Figure 1).[23] In that report, the authors propose a possible catalytic cycle, namely, the C−O oxidative addition to cobalt, followed by transmetalation and the final

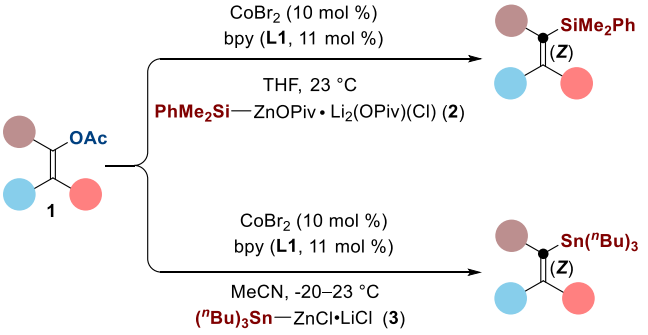

Figure 1. Cobalt-catalyzed C−O stannylation and silylation.

reductive elimination. Other potential avenues—for example, an oxidative addition-based mechanism without chelation assistance or an alkene insertion/β-acetoxy elimination pathway—have not been explored. According to previous reports, achieving C−O functionalization stereoselectively to form a single diastereoisomeric intermediate has always been the key

Received: March 31, 2023
Accepted: June 6, 2023
Published: June 16, 2023

https://doi.org/10.1021/acsomega.3c02177
ACS Omega 2023, 8, 23791−23798

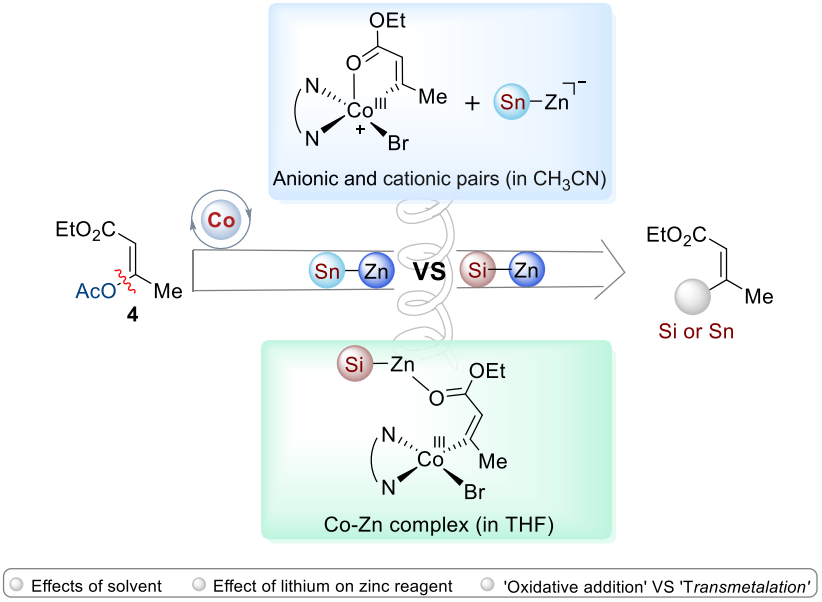

Figure 2. Cobalt-catalyzed C−O stannylation and silylation.

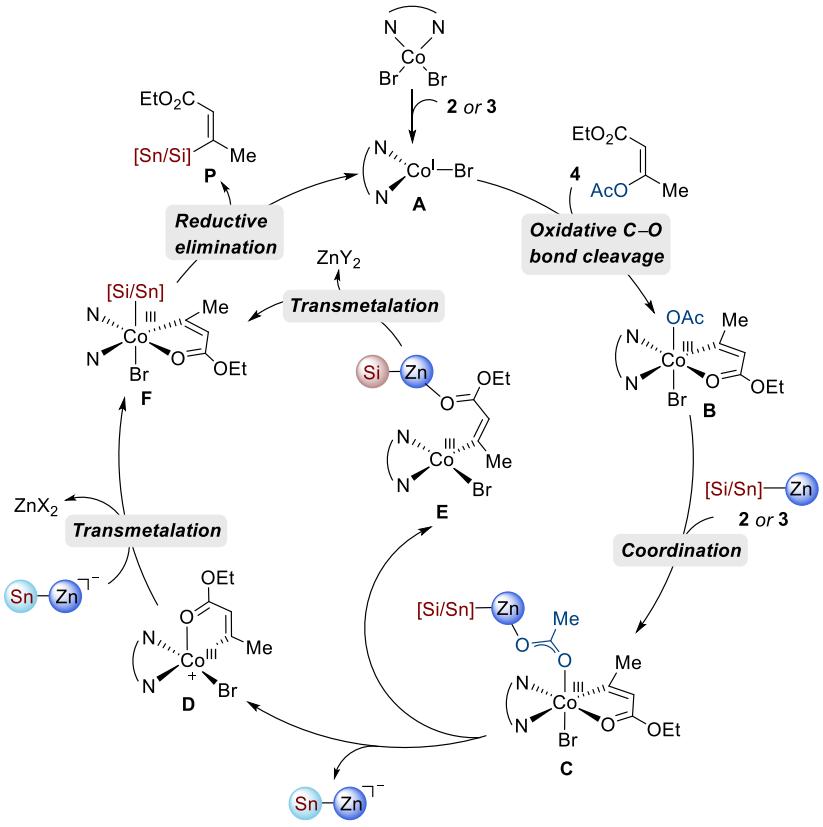

Figure 3. Plausible catalytic cycle.

step.[24] Details about the reaction mechanisms are worth investigating for all possible paths. In addition, the process of transmetalation in which a Sn− or a Si−Zn reagent participates also varies from one reaction system to another. Therefore, theoretical calculations on C−O silylation and stannylation can help us better understand the thermodynamics and kinetics of the entire reaction.[25−28]

A simplified Sn−Zn molecular model was used for theoretical investigation in a previous study.[23] Neither the effects of solvents nor the coordination of a lithium salt to Zn on both reactions was explored therein; however, these factors often play a decisive role in the reaction mechanism. Moreover, an investigation into the mechanisms of the C−O silylation process was absent in Li's work. Herein, as shown in Figure 2, the following issues were investigated in detail with DFT methods: (1) the most stable structure of Co(bpy)Br catalysts (where bpy stands for bipyridine) under different solvents, (2) the effects of solvents and lithium salts on Sn− or Si−Zn

https://doi.org/10.1021/acsomega.3c02177
ACS Omega 2023, 8, 23791−23798

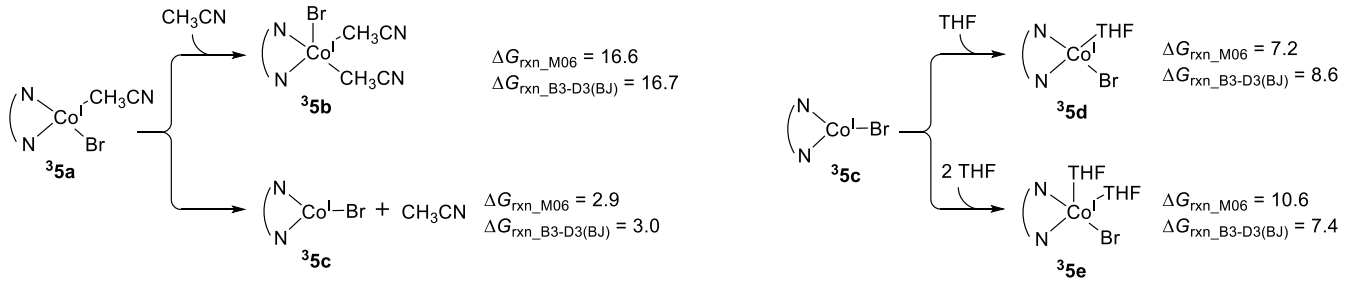

Figure 4. DFT study of the most stable structure of the Co(bpy)Br catalyst. All energies were calculated at the(U)B3LYP-D3(BJ)/6-311+G(d,p)−SDD/SMD(CH_3CN or THF)//(U)B3LYP-D3(BJ)/6-31G(d)−LANL2DZ and M06/6-311+G(d,p)−SDD/SMD(CH_3CN or THF)//(U)-B3LYP-D3(BJ)/6-31G(d)−LANL2DZ level of theory.

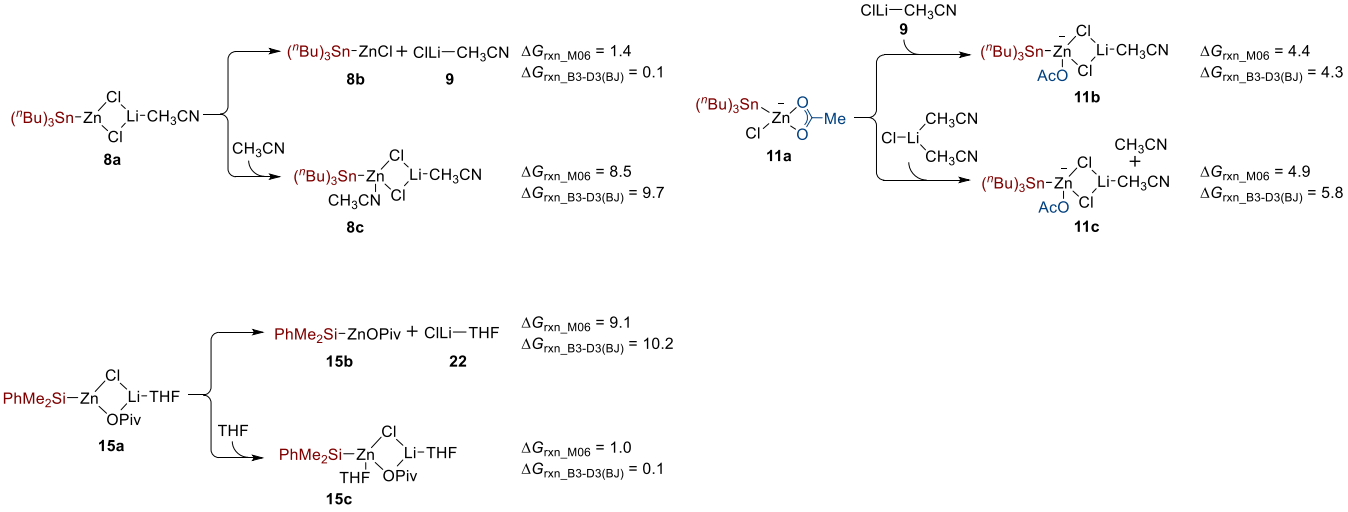

Figure 5. Structures and energies of Sn-/Si−Zn reagents calculated with M06 and B3LYP-D3(BJ) functionals.

reagents, (3) a comparison of the oxidative addition and the olefin insertion/β-acetoxy elimination mechanisms, and (4) a detailed exploration of possible pathways for the C−O silylation and stannylation reactions. We used both the popular B3LYP functional and the more accurate M06 functional in the current calculations. We believe that the current computational research will help researchers to understand the stereoselective C−O silylation and stannylation reactions better and even to inspire the investigation of similar reactions for the construction of C−Si and C−Sn bonds.

■ COMPUTATIONAL METHODS

All density functional theory (DFT) calculations were performed using the Gaussian 16 software package.[29] Geometries were optimized using the (U)B3LYP[30] functional and Grimme's D3(BJ) dispersion correction[31] with a mixed basis set of LANL2DZ for Zn, Sn, or Co and 6-31G(d) for all other atoms. In addition, we used the standard LANL2DZ effective core potential parameters for the metal atoms. Vibrational frequencies were calculated for all stationary points to confirm whether each optimized structure is a local minimum on the respective potential energy surface or a transition-state structure with only one imaginary frequency. The thermodynamic quantities under 298.15 K and 101.3 kPa were obtained with frequency calculations. Solvation energy corrections were calculated in CH_3CN or THF solvent with the SMD continuum solvation model[32] based on the gas-phase-optimized geometries. (U)-M06[33] and (U)B3LYP-D3(BJ) functionals with a mixed basis set of SDD for Zn, Sn, or Co and 6-311+G(d, p) for other atoms were used for single-point energy calculations. Furthermore, we used the standard SDD effective core potential parameters for the metal atoms. The energies obtained by the two levels of theory were compared in some key steps, and those calculation results also show that the triplet state is more stable for both Co(I) and Co(III) complexes. The optimized transition-state structures were plotted using CYLview.[34]

■ RESULTS AND DISCUSSION

Based on our mechanistic studies and previous reports on the cobalt-catalyzed cross-coupling reactions with alkenyl acetate, a plausible mechanism for the cobalt-catalyzed silylation and stannylation of alkenyl acetates **4** has been proposed, as shown in Figure 3.[35,36] The Co(II) precatalyst is initially reduced to form an active L_nCo^I−**A** species by the [Si or Sn]−[Zn] complex (**2** or **3**); the oxidative addition then breaks the bond between alkenyl acetate **4** and the C−O bond to generate intermediate **B**. The coordination between **B** and **2** or **3** leads to the formation of intermediate **C**. The transmetalation of Sn−Zn or Si−Zn could be achieved by dissociation of the zinc acetate group on **C**; the obtained cationic intermediate **D** or the neutral intermediate **E**, in which both acetyl and carbonyl groups are coordinated with Zn, then undergoes the transmetalation process to obtain intermediate **F**. The final reductive elimination of **F** releases the desired alkenyl silanes and stannanes in a stereoretentive fashion and regenerates the catalytically active cobalt species **A** to close the catalytic cycle.

https://doi.org/10.1021/acsomega.3c02177
ACS Omega 2023, 8, 23791−23798

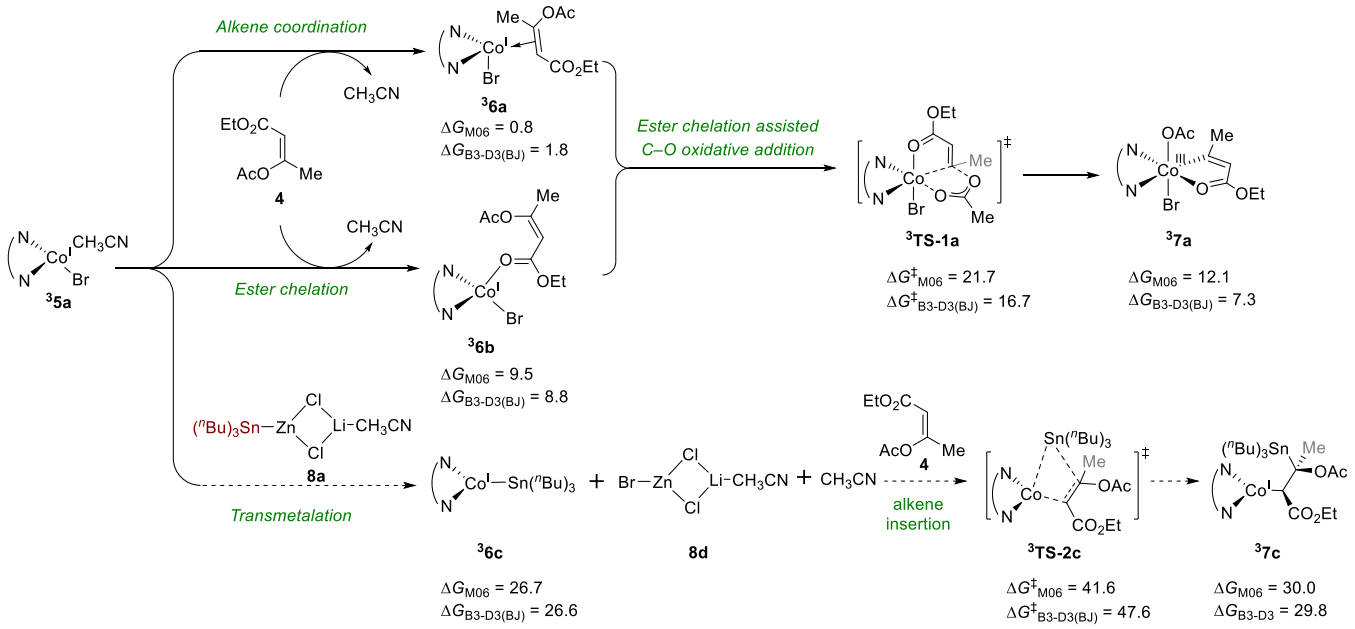

Figure 6. Oxidative−addition mechanism and the alkene insertion/β-acetoxy elimination mechanism calculated with M06 and B3LYP-D3(BJ) functionals.

Of the four issues listed in the Introduction section, we first studied the most stable structure of the Co(bpy)Br catalyst. As shown in Figure 4, when the B3-D3(BJ) functional is selected for the calculation, compound ^{3}**5a** dissociates a molecule of CH_3CN to produce Co(bpy)Br (^{3}**5c**) that is endothermic by 3.0 kcal/mol, whereas the coordination of one THF to ^{3}**5c** is endergonic by 7.4 kcal/mol. Therefore, for Sn−Zn reagents, triplet ^{3}**5a** should be selected for subsequent reactions. For Si−Zn reagents, ^{3}**5c** serves as the starting point for the subsequent reactions.

Subsequently, we explored the influence of the lithium salt and solvent coordination on Zn reagents, as shown in Figure 5. The structures of the Sn−Zn and Si−Zn reagents were carefully studied, including the coordination of the solvent (THF or CH_3CN) and the effect of the salt LiCl. When the B3-D3(BJ) functional is selected for the DFT calculation, for Sn−Zn reagents, the coordination of one molecule of CH_3CN to **8a** is endergonic by 9.7 kcal/mol, and the dissociation of **9** ($LiCl{\cdot}CH_3CN$) from **8a** is endergonic by 0.1 kcal/mol. These results indicate that the most stable Sn−Zn reagent is **8a**. In addition, the transmetalation process involved in Sn−Zn reagents is achieved by anion−cation pairing, so we also explored the structure of anionic intermediates **11**. The computational results suggest that the coordination of **9** ($LiCl{\cdot}CH_3CN$) or $LiCl{\cdot}(CH_3CN)_2$ to Zn is thermodynamically disfavored. Similarly, we have explored the most stable structure of Si−Zn reagents. The computational results show that the coordination of THF to **15a** produces **15c** that is endothermic by 0.1 kcal/mol, and the dissociation of **22** (LiCl·THF) from intermediate **15a** is endothermic by 10.2 kcal/mol. Therefore, the most stable structure of the Si−Zn reagent is **15a**. For details on the three-dimensional structure of some reactive formulas, please refer to Figure S6.

Using whether CH_3CN or THF as a solvent, the mechanism of oxidation addition is basically the same, so on the basis of the most stable Co(bpy)Br catalytic complex ^{3}**5a**, we studied the mechanism mainly of the C−O silylation oxidative addition. As shown in Figure 6, we investigated two possible pathways for the oxidative addition of ^{3}**5a** and alkenyl acetate **4**. In the first potential pathway, an alkene-coordination intermediate ^{3}**6a** was located before the C−O oxidative addition. Although this intermediate has a lower relative free energy than that of the ester-coordinated intermediate ^{3}**6b**, the formation of the following C−O oxidative addition transition state ^{3}**TS-1a** also accounts for the chelation of the ester group. The oxidative addition transition state was not observed in the absence of chelation assistance. For the second potential reaction pathway, an alkene insertion transition state ^{3}**TS-2c** was located, followed by the transmetalation of the triplet Co(I) complex ^{3}**5a** with the stannyl zinc reagent **8a** ((^{n}Bu)$_3$Sn−ZnCl·LiCl·CH_3CN). However, the activation free energy of ^{3}**TS-2c** ($\Delta G_{B3\text{-}D3(BJ)}^{\ddagger}$ = 47.6 kcal/mol) is very high, which indicates that the alkene insertion pathway is disfavored.

Based on the previous study, we first explored the reaction pathway of C−O stannylation by selecting the bulky complex **8a** ((^{n}Bu)$_3$Sn−ZnCl·LiCl·CH_3CN) for the model reaction. The cross-coupling reaction of the cobalt-catalyzed alkenyl acetates **4** was studied by the DFT method. As shown in Figure 3, the catalytic cycle starts from a cobalt(I) bromide complex.[36] Computational studies have shown that the spin state of Co(bpy)Br **5a** is a triplet, and the subsequent C−O oxidative addition to cobalt(I)[37] (via ^{3}**TS-1a**) also occurs on the triplet free-energy profile (see Figure S1 in the Supporting Information for details). The structural analysis of transition state ^{3}**TS-1a** showed that the acetoxyl group is coplanar with the bpy ligand and that the alkene is coordinated with the metal center at the apical position. These results illustrate the chelation effect during the oxidative addition of C−O (Figure 6).[38] The subsequent transmetalation of cobalt(III) acetate ^{3}**7a** from the hexa-coordinated complex is tricky because the Sn(^{n}Bu)$_3$ fraction is extremely bulky. Therefore, a stepwise pathway, consisting of acetoxy dissociation and Sn(^{n}Bu)$_3$ transmetalation, was proposed. Our computational studies reveal that upon its coordination to stannyl zinc reagent **8a**, acetoxy can dissociate from the cobalt(III) center, and lithium salt **9** ($LiCl{\cdot}CH_3CN$) can dissociate from the zinc center. The

https://doi.org/10.1021/acsomega.3c02177
ACS Omega 2023, 8, 23791−23798

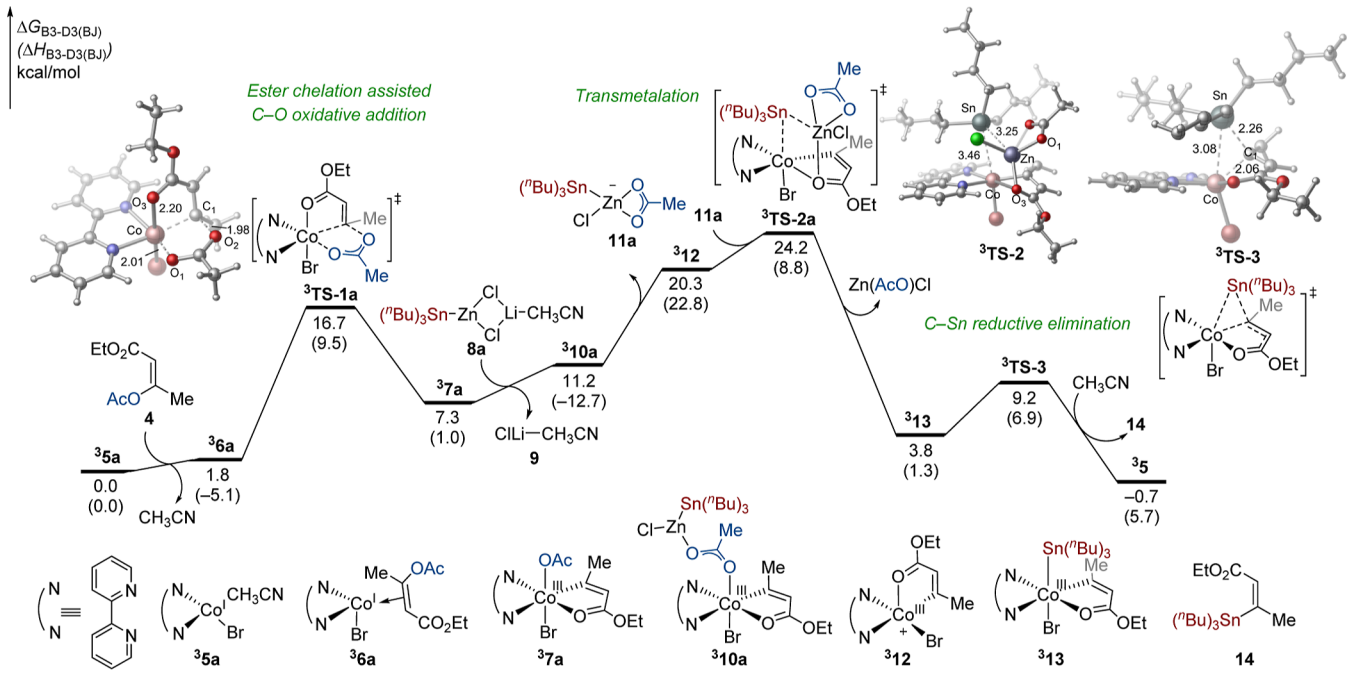

Figure 7. Free-energy profile of the cobalt(I)-catalyzed cross-coupling stannylation of C−O. Bond lengths are given in angstroms (Å).

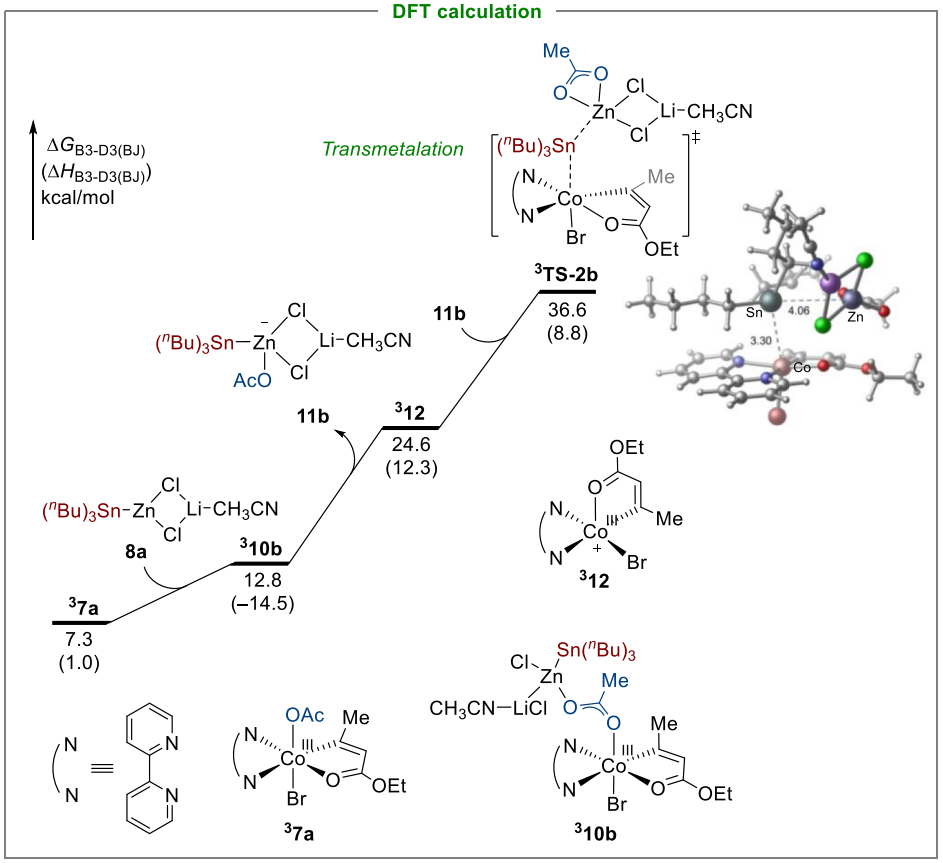

Figure 8. Effect of the LiCl·CH_3CN group (**9**) departure on the stannylation of C−O. The energies were calculated at the (U)B3LYP-D3(BJ)/6-311+G(d,p)−SDD/SMD(CH_3CN)//(U)B3LYP-D3(BJ)/6-31G(d)−LANL2DZ level of theory.

resulting zinc acetate **11a** will react with pentacoordinated cobalt(III) complex ^{3}**12**. Through the transmetalation transition state ^{3}**TS-2a**, the Sn(^{n}Bu)$_3$ moiety is partially transferred to cobalt(III) to form the octahedral cobalt(III) complex ^{3}**13**. The bond distances of Sn−Co (3.46 Å) and Sn−Zn (3.25 Å) in ^{3}**TS-2a** also reflect the large steric hindrance of the Sn(^{n}Bu)$_3$ moiety. Finally, the C−Sn reductive elimination (via ^{3}**TS-3**) leads to the formation of the stereoretentive

https://doi.org/10.1021/acsomega.3c02177
ACS Omega 2023, 8, 23791−23798

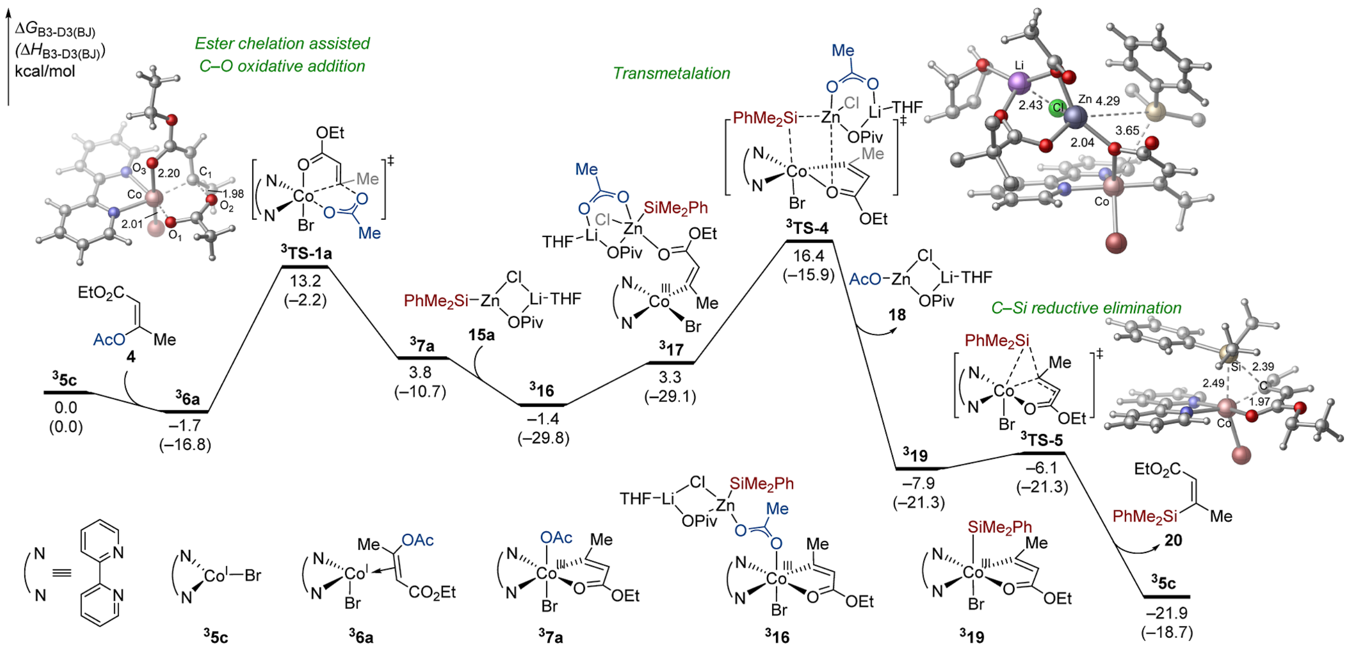

Figure 9. Free-energy profile of the cobalt(I)-catalyzed cross-coupling reaction of the alkenyl acetate **4** with **15a** ($Me_2PhSi-ZnOPiv \cdot LiCl \cdot THF$).

product **14**. Intrinsic reaction coordination (IRC) calculations have verified the reliability of these transition-state structures (see Figures S8 and S9 in the Supporting Information for details). The activation free energy of ^{3}**TS-2a** is higher than that of ^{3}**TS-1a** ($\Delta\Delta G_{B3\text{-}D3(BJ)}{}^{\ddagger}$ = 7.5 kcal/mol), which suggests that transmetalation is likely to be the rate-determining step of this reaction. In addition, the results of M06 functional calculation are placed in the Supporting Information (see Figure S2).

Although the Sn−Zn reagent **8a** has a reasonable stability, as shown in Figure 8, its low reactivity in transmetalation, indicated by the higher activation free energy (^{3}**TS-2b**, $\Delta G_{B3\text{-}D3(BJ)}{}^{\ddagger}$ = 36.6 kcal/mol), indicates that the lithium salt **9** will dissociate before transmetalation occurs. The most favored reaction pathway can be determined by combining all the data, as shown in Figure 7.

Next, we continued to study the C−O silylation with the silyl zinc reagent **2**; the calculation results were similar to those for the stannyl zinc reagent. The detailed calculations, using THF as a solvent, are shown in Figure 9. The cobalt-catalyzed cross-coupling reaction of alkenyl acetates **4** with the Si−Zn reagent **15a** was calculated. The results suggest that the spin state of Co(bpy)Br **5c** is a triplet, and the subsequent C−O oxidative addition to cobalt(I)[37] (via ^{3}**TS-1a**) also occurs on the triplet free-energy profile (see Figures S3 and S4 in the Supporting Information for details). The subsequent Si−Zn reagent **15a** and the intermediate ^{3}**7a** directly transmetallized because they contain two large groups Me_2PhSi and OPiv; the two molecules are close to each other and cause large spatial obstacles. However, unlike the pathway involving Sn−Zn reagents, a stepwise pathway consisting of acetoxy dissociation followed by Me_2PhSi transmetalation is proposed in this work. In addition, we have calculated this path to transmetalation by forming anion and cation pairs, as shown in Figure S7. Our computational studies reveal that upon the coordination to **15a**, acetoxy can dissociate from cobalt(III) to form an intermediate complex ^{3}**17**, in which both acetyl and carbonyl groups are coordinated with Zn. Through the transmetalation transition state ^{3}**TS-4**, the Me_2PhSi moiety is transferred to cobalt(III), forming the octahedral cobalt(III) complex ^{3}**19**. The bond distances of Co−Si (3.65 Å) and Zn−Si (4.29 Å) in ^{3}**TS-4** also reflect the large steric hindrance of the Me_2PhSi moiety. Finally, the C−Si reductive elimination (via ^{3}**TS-5**) leads to the formation of the stereoretentive product **20**. The activation free energy of ^{3}**TS-4** ($\Delta G_{B3\text{-}D3(BJ)}{}^{\ddagger}$ = 16.4 kcal/mol) is higher than that of ^{3}**TS-1a** ($\Delta G_{B3\text{-}D3(BJ)}{}^{\ddagger}$ = 13.2 kcal/mol), which indicates that the transmetalation is most likely the rate-determining step of this reaction. In addition, the results of M06 functional calculation are placed in the Supporting Information (see Figure S5).

■ CONCLUSIONS

In conclusion, theoretical methods were used to investigate the mechanism and influencing factors of the stereoselective C−O bond silylation and stannylation of alkenyl acetic ester catalyzed by cobalt. Detailed mechanistic studies strongly suggest that the stereoselectivity is caused by chelation-assisted oxidative addition of cobalt to the C−O bond of alkenyl acetates and that the transmetalation is most likely the rate-determining step. In addition, for Sn−Zn reagents, the transmetalation process was achieved by anion and cation pairs, whereas for Si−Zn reagents, the process involved Co−Zn complexes. Moreover, the free energy profile indicates that the energy calculated by the M06 method is increased compared with the results of the B3LYP-D3(BJ) calculation, especially for the transmetalation process, which has a pronounced influence on the Si−Zn reagent. We believe that our current computational studies will inspire experimental chemists to investigate similar reactions of C−Si and C−Sn complexes, thereby further expanding the applications of Si- and Sn-containing compounds in organic synthesis, materials chemistry, and medicine.

https://doi.org/10.1021/acsomega.3c02177
ACS Omega 2023, 8, 23791−23798

■ ASSOCIATED CONTENT

Supporting Information

The Supporting Information is available free of charge at https://pubs.acs.org/doi/10.1021/acsomega.3c02177.

Singlet free energy profile of C−O silylation and stannylation reactions, energy profile calculated by the M06 functional, three-dimensional structure information of the zinc reagent, atomic coordinates, and other information in this study (PDF)

■ AUTHOR INFORMATION

Corresponding Author

Cheng-Xing Cui − *School of Chemistry and Chemical Engineering, Institute of Computational Chemistry, Henan Institute of Science and Technology, Xinxiang, Henan 453003, P. R. China; ZhengZhou JiShu Institute of AI Science, Zhengzhou, Henan 451162, P. R. China;* orcid.org/0000-0001-9632-5798; Email: chengxingcui@hist.edu.cn

Authors

Jiali Peng − *School of Chemistry and Chemical Engineering, Institute of Computational Chemistry, Henan Institute of Science and Technology, Xinxiang, Henan 453003, P. R. China; Engineering Research Center of Organosilicon Compounds & Materials, Ministry of Education, College of Chemistry and Molecular Sciences, Wuhan University, Wuhan, Hubei 430072, P. R. China*

Jun Jiang − *ZhengZhou JiShu Institute of AI Science, Zhengzhou, Henan 451162, P. R. China; Hefei National Laboratory for Physical Sciences at the Microscale, Collaborative Innovation Center of Chemistry for Energy Materials, School of Chemistry and Materials Science, University of Science and Technology of China, Hefei, Anhui 230026, P. R. China;* orcid.org/0000-0002-6116-5605

Complete contact information is available at: https://pubs.acs.org/10.1021/acsomega.3c02177

Notes

The authors declare no competing financial interest.

■ ACKNOWLEDGMENTS

The authors acknowledge the financial support from the Funding for Internationalization Training of High-Level Talent in Henan Province and the Open Project of ZhengZhou JiShu Institute of AI Science (ZZJSA2023001).

■ REFERENCES

(1) Ojima, I. *The Chemistry of Organic Silicon Compounds*; Patai, S., Rappoport, Z., Eds.; Wiley: Chichester, 1989.

(2) Franz, A. K.; Wilson, S. O. Organosilicon Molecules with Medicinal Applications. *Med. Chem.* **2013**, *56*, 388−405.

(3) Xue, W.; Shishido, R.; Oestreich, M. Bench-Stable Stock Solutions of Silicon Grignard Reagents: Application to Iron- and Cobalt-Catalyzed Radical C(sp^3)−Si Cross-Coupling Reactions. *Angew. Chem., Int. Ed.* **2018**, *57*, 12141−12145.

(4) Bähr, S.; Xue, W.; Oestreich, M. C(sp^3)−Si Cross-Coupling. *ACS Catal.* **2019**, *9*, 16−24.

(5) Ni, D.; Brown, M. K. Three-Component Ni-Catalyzed Silylacylation of Alkenes. *ACS Catal.* **2021**, *11*, 1858−1862.

(6) Levent, E.; Sala, O.; Wilm, L. F. B.; Löwe, P.; Dielmann, F. Heterobimetallic complexes composed of bismuth and lithium carboxylates as polyurethane catalysts − alternatives to organotin compounds. *Green Chem.* **2021**, *23*, 2747−2755.

(7) Engels, H. W.; Pirkl, H. G.; Albers, R.; Albach, R. W.; Krause, J.; Hoffmann, A.; Casselmann, H.; Dormish, J. Polyurethane: vielseitige Materialien und nachhaltige Problemlöser für aktuelle Anforderungen. *Angew. Chem.* **2013**, *125*, 9596−9616.

(8) Noh, H. J.; Sadhasivam, T.; Han, M.; Lee, K.; Kim, J. Y.; Jung, H. Y. Investigations of $FeCl_3$ adducted N-heterocyclic carbene complex as curing-delayed action catalyst for polyurethane polymerization. *J. Catal.* **2020**, *382*, 77−85.

(9) Peris, E. Smart N-Heterocyclic Carbene Ligands in Catalysis. *Chem. Rev.* **2018**, *118*, 9988−10031.

(10) Kim, S.-S.; Senthil, C.; Jung, S. M.; Jung, H. Y. Chemically engineered alloy anode enabling fully reversible conversion reaction: design of a C−Sn bonded aerofilm anode. *J. Mater. Chem. A* **2022**, *10*, 3595−3604.

(11) *Metal-Catalyzed Cross-Coupling Reactions and More*; de Meijere, A., Bräse, S., Oestreich, M., Eds.; Wiley, 2014.

(12) Haas, D.; Hammann, J. M.; Greiner, R.; Knochel, P. Recent developments in negishi cross-coupling reactions. *ACS Catal.* **2016**, *6*, 1540−1552.

(13) Campeau, L. C.; Hazari, N. Cross-Coupling and Related Reactions: Connecting Past Success to the Development of New Reactions for the Future. *Organometallics* **2019**, *38*, 3−35.

(14) Qiu, Z.; Li, C.-J. Transformations of Less-Activated Phenols and Phenol Derivatives via C−O Cleavage. *Chem. Rev.* **2020**, *120*, 10454−10515.

(15) Nassar, Y.; Rodier, F.; Ferey, V.; Cossy, J. Cross-Coupling of Ketone Enolates with Grignard and Zinc Reagents with First-Row Transition Metal Catalysts. *ACS Catal.* **2021**, *11*, 5736−5761.

(16) Haas, D.; Hammann, J. M.; Greiner, R.; Knochel, P. Recent developments in negishi cross-coupling reactions. *ACS Catal.* **2016**, *6*, 1540−1552.

(17) Guo, P.; Zhan, M. Iridium-Catalyzed Enantioconvergent Allylation of a Boron-Stabilized Organozinc Reagent. *J. Org. Chem.* **2021**, *86*, 9905−9913.

(18) Suzuki, K.; Sugihara, N.; Nishimoto, Y.; Yasuda, M. anti-Selective Borylstannylation of Alkynes with (o-Phenylenediaminato) borylstannanes by a Radical Mechanism. *Angew. Chem., Int. Ed.* **2022**, *61*, No. e202201883.

(19) Wang, J.; Duan, Z.; Liu, X.; Dong, S.; Chen, K.; Li, J. Salt-Stabilized Silylzinc Pivalates for Nickel-Catalyzed Carbosilylation of Alkenes. *Angew. Chem., Int. Ed.* **2022**, *61*, No. e202202379.

(20) Cheng, X.; Liu, X.; Wang, S.; Hu, Y.; Hu, B.; Lei, A.; Li, J. Organozinc pivalates for cobalt-catalyzed difluoroalkylarylation of alkenes. *Nat. Commun.* **2021**, *12*, 4366.

(21) Han, S.; Liu, S.; Liu, L.; Ackermann, L.; Li, J. Cobalt-Catalyzed Diastereoselective Difluoroalkylation/Giese Addition Domino Reactions. *Org. Lett.* **2019**, *21*, 5387−5391.

(22) Li, J.; Tan, E.; Keller, N.; Chen, Yi-H.; Zehetmaier, P. M.; Jakowetz, A. C.; Bein, T.; Knochel, P. Cobalt-Catalyzed Electrophilic Aminations with Anthranils: An Expedient Route to Condensed Quinolines. *J. Am. Chem. Soc.* **2019**, *141*, 98−103.

(23) Hu, Y.; Peng, J.; Hu, B.; Wang, J.; Jing, J.; Lin, J.; Liu, X.; Qi, X.; Li, J. Stereoselective C−O silylation and stannylation of alkenyl acetates. *Nat. Commun.* **2023**, *14*, 1454.

(24) Hu, Y.; Hu, B.; Liu, X.; Ren, Z.; Li, J. Recent developments in catalytic cross-couplings with unsaturated carboxylates. *Org. Biomol. Chem.* **2021**, *19*, 7754−7767.

(25) Wang, B.; Zhang, Q.; Jiang, J.; Yu, H.; Fu, Y. Mechanistic Study on Nickel-Catalyzed Silylation of Aryl Methyl Ethers. *Chem.—Eur. J.* **2017**, *23*, 17249−17256.

(26) Chen, P.-P.; Zhang, H.; Cheng, B.; Chen, X.; Cheng, F.; Zhang, S.-Q.; Lu, Z.; Meng, F.; Hong, X. How Solvents Control the Stereospecificity of Ni-Catalyzed Miyaura Borylation of Allylic Pivalates. *ACS Catal.* **2019**, *9*, 9589−9598.

(27) Chen, W. W.; Fernández, N. P.; Baranda, M. D.; Cunillera, A.; Rodríguez, L. G.; Shafir, A.; Cuenca, A. B. Exploring benzylic gem-

C(sp3)−boron−silicon and boron−tin centers as a synthetic platform. *Chem. Sci.* **2021**, *12*, 10514−10521.
(28) Lu, C.; Lin, Y.; Wang, M.; Zhou, J.; Wang, S.; Jiang, H.; Kang, K.; Huang, L. Nickel-Catalyzed Ring-Opening of Benzofurans for the Divergent Synthesis of ortho-Functionalized Phenol Derivatives. *ACS Catal.* **2023**, *13*, 2432−2442.
(29) Frisch, M. J.; Trucks, G. W.; Schlegel, H. B.; Scuseria, G. E.; Robb, M. A.; Cheeseman, J. R.; Scalmani, G.; Barone, V.; Mennucci, B.; Petersson, G. A.; Nakatsuji, H.; Caricato, M.; Li, X.; Hratchian, H. P.; Izmaylov, A. F.; Bloino, J.; Zheng, G.; Sonnenberg, J. L.; Hada, M.; Ehara, M.; Toyota, K.; Fukuda, R.; Hasegawa, J.; Ishida, M.; Nakajima, T.; Honda, Y.; Kitao, O.; Nakai, H.; Vreven, T.; Montgomery, J. A.; Peralta, J. E.; Ogliaro, F.; Bearpark, M.; Heyd, J. J.; Brothers, E.; Kudin, K. N.; Staroverov, V. N.; Kobayashi, R.; Normand, J.; Raghavachari, K.; Rendell, A.; Burant, J. C.; Iyengar, S. S.; Tomasi, J.; Cossi, M.; Rega, N.; Millam, N. J.; Klene, M.; Knox, J. E.; Cross, J. B.; Bakken, V.; Adamo, C.; Jaramillo, J.; Gomperts, R.; Stratmann, R. E.; Yazyev, O.; Austin, A. J.; Cammi, R.; Pomelli, C.; Ochterski, J. W.; Martin, R. L.; Morokuma, K.; Zakrzewski, V. G.; Voth, G. A.; Salvador, P.; Dannenberg, J. J.; Dapprich, S.; Daniels, A. D.; Farkas, O.; Foresman, J. B.; Ortiz, J. V.; Cioslowski, J.; Fox, D. J. *Gaussian 16*, Revision C.01; Gaussian, Inc.: Wallingford, CT, 2016.
(30) (a) Becke, A. D. Density-functional thermochemistry. III. The role of exact exchange. *J. Chem. Phys.* **1993**, *98*, 5648−5652. (b) Lee, C.; Yang, W.; Parr, R. G. Development of the Colle-Salvetti correlation-energy formula into a functional of the electron density. *Phys. Rev. B* **1988**, *37*, 785−789.
(31) (a) Grimme, S.; Antony, J.; Ehrlich, S.; Krieg, H. A consistent and accurate *ab initio* parametrization of density functional dispersion correction (DFT-D) for the 94 elements H-Pu. *J. Chem. Phys.* **2010**, *132*, 154104. (b) Grimme, S.; Ehrlich, S.; Goerigk, L. Effect of the damping function in dispersion corrected density functional theory. *J. Comput. Chem.* **2011**, *32*, 1456−1465.
(32) Marenich, A. V.; Cramer, C. J.; Truhlar, D. G. Universal Solvation Model Based on Solute Electron Density and on a Continuum Model of the Solvent Defined by the Bulk Dielectric Constant and Atomic Surface Tensions. *J. Phys. Chem. B* **2009**, *113*, 6378−6396.
(33) Zhao, Y.; Truhlar, D. G. The M06 suite of density functionals for main group thermochemistry, thermochemical kinetics, noncovalent interactions, excited states, and transition elements: two new functionals and systematic testing of four M06-class functionals and 12 other functionals. *Theor. Chem. Acc.* **2008**, *120*, 215−241.
(34) Legault, C. Y. *CYLView, 1.0b*; Université de Sherbrooke: Canada, 2009. http://www.cylview.org.
(35) Rozenel, S. S.; Padilla, R.; Arnold, J. Chemistry of Reduced Monomeric and Dimeric Cobalt Complexes Supported by a PNP Pincer Ligand. *Inorg. Chem.* **2013**, *52*, 11544−11550.
(36) Qi, X.; Liu, X.; Qu, L. B.; Liu, Q.; Lan, Y. Mechanistic insight into cobalt-catalyzed stereodivergent semihydrogenation of alkynes: The story of selectivity control. *J. Catal.* **2018**, *362*, 25−34.
(37) Zhang, X.; Wang, J.; Yang, S. D. Enantioselective Cobalt-Catalyzed Reductive Cross-Coupling for the Synthesis of Axially Chiral Phosphine−Olefin Ligands. *ACS Catal.* **2021**, *11*, 14008−14015.
(38) Rogge, T.; Oliveira, J. C. A.; Kuniyil, R.; Hu, L.; Ackermann, L.; Ackermann, L. Reactivity-Controlling Factors in Carboxylate-Assisted C−H Activation under 4d and 3d Transition Metal Catalysis. *ACS Catal.* **2020**, *10*, 10551−10558.

NOTE ADDED AFTER ASAP PUBLICATION

This paper originally published ASAP on June 16, 2023. A corrected Supporting Information file was uploaded, and a new version reposted on June 23, 2023.

https://doi.org/10.1021/acsomega.3c02177
ACS Omega 2023, 8, 23791−23798